Metabolite-based Wavelets for Analyzing Magnetic Resonance Spectroscopic Signals

C. Lemke*, A. Schuck Jr.*, J-P. Antoine*, D.M. Sima† and M.I. Osorio Garcia†
*Institut de recherche en mathématiques et physique
Université catholique de Louvain, B-1348 Louvain-la-Neuve, Belgium
Email: see http://www.fyma.ucl.ac.be/people
†Department of Electrical Engineering ESAT-SCD
Katholieke Universiteit Leuven, Kasteelpark Arenberg 10, B 3001 Leuven-Heverlee, Belgium.
Email: diana.sima@esat.kuleuven.be

***Abstract*—We analyze Magnetic Resonance Spectroscopic signals by the continuous wavelet transform. Instead of the standard (Morlet) wavelet, we introduce a new class of wavelets, derived from the metabolite data themselves, using the properly normalized autocorrelation function of each signal. This allows to detect without ambiguity the presence of a given metabolite in a signal consisting of many different components.**

I. Introduction

Magnetic Resonance Spectroscopy (MRS) is a unique non-invasive tool for detecting metabolites and quantifying their concentrations through the amplitude of these contributions in the time domain. However, the MRS signal acquired at short echo-time contains contributions not only from metabolites, but also from water and macromolecules and lipids. In this paper, we apply the wavelet analysis to the MRS signals, with the aim of detecting the presence of specific metabolites in an arbitrary superposition. Analyzing in the time and scale domains simultaneously can provide more useful information than the Fourier transform, which gives only spectral information. In addition, a small perturbation of a signal which may occur during the data acquisition will result only in a small, local modification of the wavelet transform. Among several types of wavelet transforms, the continuous wavelet transform (CWT) technique [1], [2] can estimate the frequency and amplitude of the spectral line directly from the phase and modulus of the wavelet transform. A review of this approach may be found in [3].

However, the formalism developed in that paper used exclusively the Morlet wavelet transform to analyze the MRS signals. Now it is a well-known rule of the thumb that the more *a priori* information on the signal is used, the more efficient the CWT becomes. In this paper, we push that rationale to the extreme, namely, we construct dedicated wavelets directly from the MRS data themselves. The idea is to define the wavelet by the autocorrelation function of the signal, properly averaged to zero. We will proceed in two stages. In a first step, we start from a model FID signal, for instance a truncated Lorentzian (i.e. put to zero for times $t < 0$) and evaluate its performance. Then, in a second step, we start from real metabolite data. Here we face the additional problem that data are by necessity discrete, and thus also their autocorrelation function. Therefore an extra step, based on interpolation, is needed for using such discrete wavelets for a *continuous* wavelet transform. The outcome is that these wavelets look promising for the analysis of MRS signals. In particular, they are able to detect without ambiguity the presence of a given metabolite in a superposition of several metabolites and/or lipids.

II. Autocorrelation wavelets

As we said before, the idea is to start from the autocorrelation function of a given model signal and use it as adapted wavelet after proper normalization. The autocorrelation function estimator $R_{xx}(t)$ of an ergodic process time series $x(\tau)$ is defined by

$$R_{xx}(t) = \int_{-\infty}^{\infty} x(\tau)\overline{x(\tau - t)}\,\mathrm{d}\tau \tag{1}$$

where the overline denotes the complex conjugate [4]. After subtracting the mean,

$$\psi_x(t) = R_{xx}(t) - \mathrm{E}\{R_{xx}\}, \tag{2}$$

we obtain an admissible wavelet $\psi(t)$ (provided the mean $\mathrm{E}\{R_{xx}\}$ is finite).

Now we apply this technique to a modified Lorentzian spectral line

$$x_1(t) = Ae^{-Dt}e^{i\omega_0 t}\,\theta(t),\ D > 0, \tag{3}$$

where $\theta(t)$ is the Heaviside function (or step function). This model allows us to find an autocorrelation function, whereas the "pure" Lorentzian spectral line cannot have an analytical autocorrelation function. Also this model looks more like the FID signals obtained *in vitro* than a pure Lorentzian one. Now, computing the autocorrelation function of x_1 by (1), we obtain the adapted wavelet

$$\psi(t) = \frac{A}{2D}e^{-D|t|+i\omega_0 t},\ -\infty < t < \infty, \tag{4}$$

with Fourier transform

$$\Psi(\omega) = \frac{A^2}{D^2 + (\omega - \omega_0)^2}. \tag{5}$$

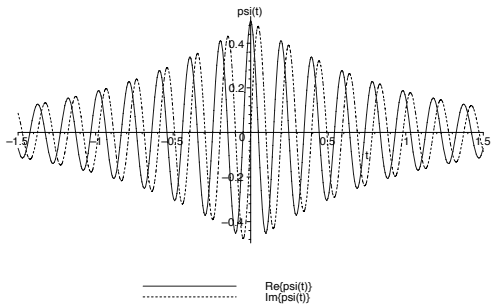

Fig. 1: $\psi(t)$, for $A = 1$, $D = 1$ and $\omega_0 = 32$ rad/s: real part (line) and imaginary part (dash).

Strictly speaking, one ought to introduce an additive correction term for making this wavelet admissible. However, as for the Morlet wavelet, too, the correction term is numerically negligible for realistic values of the parameters here, so we will omit it. We show in Fig. 1 the real part (continuous line) and the imaginary part (dashed line) of $\psi(t)$, respectively, for $A = 1$, $D = 1$ and $\omega_1 = 32$ rad/s.

The next step is to calculate the CWT of a signal s with the wavelet ψ, that is,

$$S(b,a) = \frac{1}{\sqrt{a}} \int_{-\infty}^{\infty} \overline{\psi\left(\frac{t-b}{a}\right)}\, s(t)\, \mathrm{d}t \tag{6}$$

$$= \frac{1}{2\pi}\sqrt{a} \int_{-\infty}^{\infty} \overline{\Psi(a\omega)}\, S(\omega)\, e^{i\omega b}\, \mathrm{d}\omega\,. \tag{7}$$

Here $S(\omega)$ is the Fourier transform of $s(t)$, whereas $a > 0$ and $b \in \mathbb{R}$ are the scaling and translation variables, respectively.

Applying these formulas to the x_1 signal itself, one finds that the CWT diverges as $a \to 1$ (the match between the wavelet and the signal is too perfect!). This behavior changes, however, if we analyze numerically a signal limited in time, like $Ae^{-Dt}e^{i\omega_0 t}$, $0 \leqslant t \leqslant T_0$, for some finite T_0. For the discretized signal, we take:

$$x_1[n] = \begin{cases} 0, & 0 \leqslant n \leqslant \frac{N}{2} - 1, \\ A\, e^{-D(n-\frac{N}{2})t_s}\, e^{i\omega_0(n-\frac{N}{2})t_s}, & \frac{N}{2} \leqslant n \leqslant N-1, \end{cases}$$

where t_s is the sampling period in seconds. Then we compute its CWT using the discretized version of (5). The result, shown in Fig. 2, exhibits a strong horizontal ridge (line of local maxima) for $a = 1$. The occurrence of this local maximum indicates that the component x_1 is present in the signal. This feature will be the crucial ingredient for detecting a given signal (pure metabolite) in an unknown superposition, as we will discuss in the next section.

This method can be further generalized to multipeak signals, that would be well adapted for identifying doublets or triplets, for instance, from complicated MRS spectra.

III. Metabolite-based wavelets

Now we turn to real life signals and apply the method developed above. We derive our metabolite-based wavelets

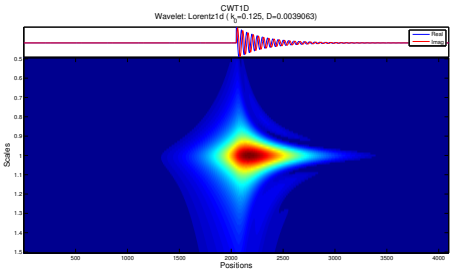

Fig. 2: $(a)|CWTx_1[n]|$ for $A = 1$, $D = 1$, $\omega_0 = 32$ rad/s, $n = [1, 4096]$ and $a = [0.5, 1.5]$ using the wavelet ψ.

from metabolite profiles, which could have been acquired by MRS measurements of phantoms filled with single metabolites or by simulation in jMRUI [6]. Each of those wavelets is supposed to be sensitive to one metabolite. It is thus necessary to construct mother wavelets with spectral characteristics similar to the ones of a certain metabolite. Therefore, we calculate the autocorrelation function of the metabolite profile $\phi_i(t)$:

$$R_i(t) = \int_{-\infty}^{\infty} \phi_i(\tau)\, \overline{\phi_i(\tau - t)}\, \mathrm{d}\tau. \tag{8}$$

In this formula, the overline indicates the complex conjugate and $i = 1, \ldots, K$ refers to the index of a certain metabolite profile out of a number of K profiles.

As the metabolite profile ϕ_i in MRS is a mixture of decaying, complex oscillations, its autocorrelation values are complex, too. The magnitude increases from zero to the maximum before it decreases again. After subtracting the mean,

$$\psi_i(t) = R_i(t) - \mathrm{E}\{R_i\}, \tag{9}$$

we obtain an admissible wavelet $\psi_i(t)$ (provided the mean $\mathrm{E}\{R_i\}$ is finite). Fig. 3 shows an example wavelet. It has been derived from an *in vitro* Creatine (Cre) profile (Fig. 3a). The resulting Cre-based wavelet shows also two characteristic peaks like the original Creatine profile in the frequency domain (Fig. 3b). In the time domain, however, the function is symmetrical with zero mean (Fig. 3c) as required for an admissible wavelet. Next, we perform the same operation for eight metabolites and two lipids contained in the data base obtained at ESAT, K.U.Leuven. These metabolite signals have been quantum mechanically simulated with NMRSCOPE [7] using a PRESS sequence, an echo time of 30 ms, and a field strength of 1.5T. Among these signals, we will present here three representative cases, N-Acetyl Aspartate (NAA), Creatine (Cre) and Lactate (Lac).

Now we face a problem. Indeed, the outcome of measurements consists only of discrete data sets for the metabolite profiles.

In order to perform the continuous wavelet transform, we need to dilate our constructed wavelets. To do that we used an Upsampler - Downsampler digital system presented in [8]. In this system, we first expand the signal by an integer factor

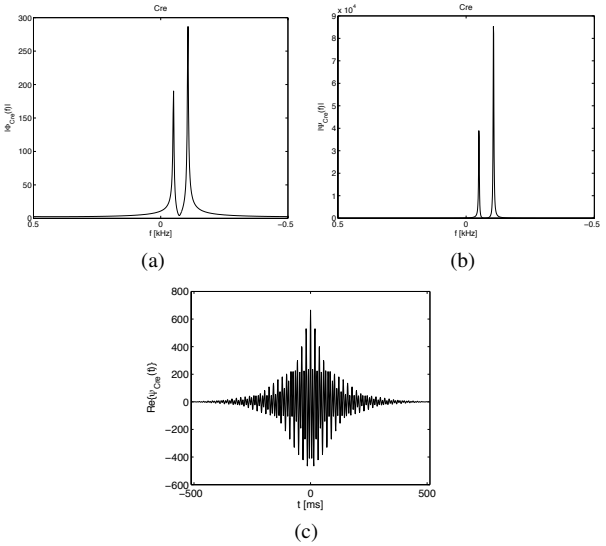

(a) (b) (c)

Fig. 3: Wavelet constructed from Creatine (Cre) in vitro profile: (a) Modulus of the Cre profile spectrum; (b) Cre-based wavelet spectrum; and (c) Real part of the Cre-based wavelet in time domain.

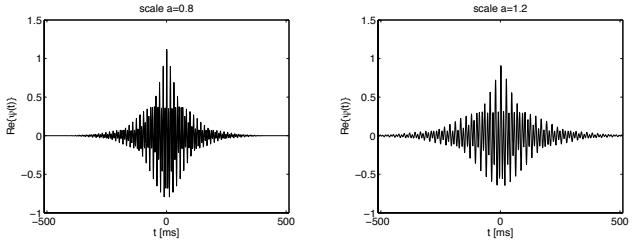

(a) (b)

Fig. 4: Cre-based wavelet at (a) scale $a = 0.8$ and (b) $a = 1.2$.

L by inserting $L - 1$ zeros between the original samples and then interpolating these values by a low-pass digital filter with cutoff frequency of π/L rad, implemented by a Bartlett window of length $2L - 1$. Next we reduce the signal by an integer factor M, filtering it by a low-pass filter with cutoff frequeny of π/M, in order to avoid aliasing and then, decimating it, i.e., keeping one sample of M samples). The filter used here was a 128 tap FIR filter designed using the MATLAB© function FIR1. With this procedure, our possible scales will be $a = L/M$. For our previous example of the Cre-based wavelet, we look at two different scales to show the effect. The time domain version at scale $a = 0.8$ and $a = 1.2$ can be seen in Figs. 4a and 4b, respectively.

In order to estimate the efficiency of the method, we will use a synthetic signal, shown in Fig. 5a, composed of all metabolites and lipids available from the data base. On the other hand, Fig. 5b shows exactly the same signal, but with the Lactate removed. The difference between the two spectra can be hardly seen. So, it is interesting to see what the metabolite-based wavelets can find in these signals. We will test the three metabolite-based wavelets, namely, the NAA-, Cre- and

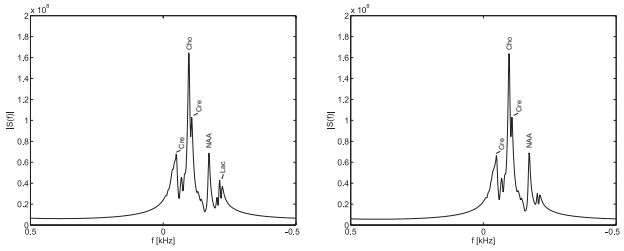

(a) (b)

Fig. 5: Example of a composed *in vivo* MRS signal: (a) including all metabolites from the data base; (b) the same as (a), but with the Lac contribution removed.

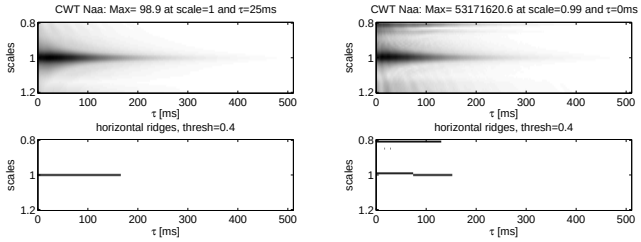

(a) (b)

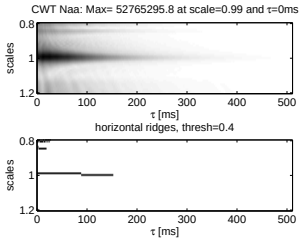

(c)

Fig. 6: CWT using the NAA-wavelet on (a) a pure NAA reference signal; (b) on the composed signal from Fig. 5a; and (c) on the composed signal from Fig. 5b. The presence of NAA is indicated by the local maxima at scale $a = 1$.

Lac-wavelets on the pure metabolite signals and on the two composed signals of Fig. 5. The upper panel of each figure shows the CWT coefficients in a time-scale representation. The lower panel shows the horizontal ridges as an indicator of local maxima of the coefficients along the time axis.

Let us begin with NAA. The CWT using the NAA-based wavelet on the pure NAA-reference signal (Fig. 6a) shows a clear line of maxima at scale $a = 1$. We find a similar line when we look at the wavelet transform using the NAA-based wavelet on the composed signal (Fig. 6b). While we see some effects on lower scales, we have clear maxima values at scale $a = 1$ again, which indicate the presence of NAA in the analysed signal. Exactly the same behavior is observed on the composed signal without Lac (Fig. 6c).

Next, we do the same analysis with Cre. So, we apply the Cre-based wavelet on a Cre reference signal. The result is shown in Fig. 7a. The outcome is not a straight line as with NAA before. However, it still shows significant local maxima

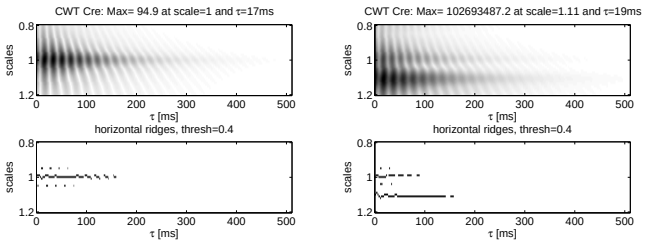

(a) (b)

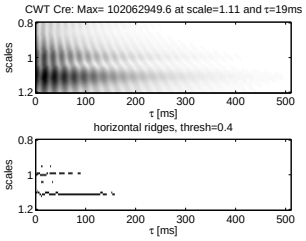

(c)

Fig. 7: CWT using the Cre-wavelet on (a) a pure Cre reference signal; (b) on the composed signal from Fig. 5a; and (c) the same without Lac. The presence of Cre is indicated by the local maxima at scale $a = 1$.

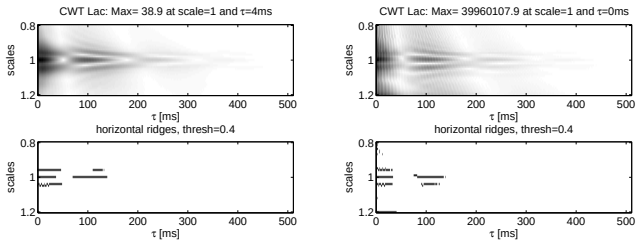

(a) (b)

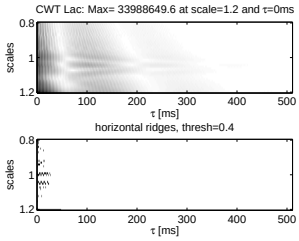

(c)

Fig. 8: CWT using the Lac-wavelet on (a) a pure Lac reference signal and (b) on the composed signal from Fig. 5a. The presence of Lac is indicated by the local maxima at scale $a = 1$ both in (a) and in (b), but not in (c), since Lac is not included in this composed signal.

at scale $a = 1$, which are characteristic for this metabolite. We find that structure again at scale $a = 1$ if we apply the Cre-based wavelet on our composed signal (see Fig. 7b). Although we see again local maxima arising at other scales, too, we still can tell from that image that Cre is present in the signal. Again the same result is obtained on the composed signal without Lac, there are only some minor differences in the amplitudes of the maximum CWT magnitude (Fig. 7c).

Finally we turn to the Lac-wavelet. The Lac-based wavelet shows for both the Lac reference signal and the composed signal a wavelet transform with a significant structure at scale $a = 1$ (Figs. 8a and 8b). Again, this is how the presence of Lac in the composed signal is indicated. When we analyze the composed signal without Lac, however, that structure at scale $a = 1$ disappears as it should, since the metabolite is absent (Fig. 8c).

IV. Conclusion

The conclusion of the preceding analysis is that these metabolite-based wavelets are able to identify without ambiguity the presence of the corresponding metabolite in a composed signal, simply by viewing local maxima in the wavelet transform. In addition, using an approximate expression for the wavelet spectrum of a composed signal, these wavelets allow us also to estimate the amplitude of each metabolite contained in the mixture. This aspect, however, requires further work, as well as designing a fully automated algorithm based on the present technique.

Acknowledgment

This work is part of the Advanced Signal Processing for Ultra-fast Magnetic Resonance (FAST) project funded by the Marie-Curie Research Network (MRTN-CT-2006-035801) http://fast-mrs.eu. A. Schuck Jr. thanks the Conselho Nacional de Pesquisa e Desenvolvimento - CNPq, Brazil, for its financial support. The authors would also like to express their gratitude to Prof. S. van Huffel (K.U. Leuven) and Prof. D. van Ormondt (TU Delft) for their invaluable advice.

References

[1] P. Guillemain, R. Kronland-Martinet, and B. Martens, Estimation of spectral lines with the help of the wavelet transform, applications in NMR spectroscopy. In Y. Meyer, editor, *Wavelets and Applications — Proc. Int. Conf. Marseille, France, May 1989*, pp. 38–60, Masson, Paris, and Springer, Berlin, 1992.

[2] N. Delprat, B. Escudié, P. Guillemain, R. Kronland-Martinet, P. Tchamitchian, and B. Torrésani, Asymptotic wavelet and Gabor analysis extraction of instantaneous frequencies. *IEEE Transactions on Information Theory*, 38(2): 644–664, 1992.

[3] A. Suvichakorn, H. Ratiney, A. Bucur, S. Cavassila, and J-P. Antoine, Toward a quantitative analysis of *in vivo* magnetic resonance proton spectroscopic signals using the continuous Morlet wavelet transform, *Meas. Sci. Technol.* 20, paper #104029 (11 pages), 2009.

[4] A. Papoulis and S.U. Pillai, *Probability, Random Variables and Stochastic Processes*. McGraw-Hill, NY, 4th edition, 2002.

[5] L. Jacques, A. Coron, P. Vandergheynst, and A. Rivoldini, The YAWTb toolbox : Yet Another Wavelet Toolbox, 2007. http://rhea.tele.ucl.ac.be/yawtb.

[6] For the MRUI Project, see http://sermn02.uab.cat/mrui/mrui_Overview.shtml

[7] D. Graveron-Demilly, A. Diop, A. Briguet, and B. Fenet, Product-operator algebra for strongly coupled spin systems, *J. Magn. Reson. A*, 101(3): 233?239, 1993.

[8] A. Oppenheim, R.W.Schaffer, and J.R. Buck *Discrete-Time Signal Processing*. Prentice-Hall, Englewood Cliffs, NJ, 2nd edition, 1999.